K channel gating by an affinity-switching selectivity filter

Antonius M. J. VanDongen*

Department of Pharmacology, Duke University, Durham, NC 27710

Communicated by Lutz Birnbaumer, National Institutes of Health, Research Triangle Park, NC, December 31, 2003 (received for review December 5, 2003)

A universal property of ion channels is their ability to alternate stochastically between two permeation states, open and closed. This behavior is thought to be controlled by a steric ''gate'', a structure that physically impedes ion flow in the closed state and moves out of the way during channel opening. Experiments employing macroscopic currents in the *Shaker* K channel have suggested a cytoplasmic localization for the gate. Crystallographic structures of the KcsA K channel indeed reveal a cytoplasmic constriction, implying that the gate and selectivity filter are localized to opposite ends of the permeation pathway. However, analysis of K channel subconductance behavior has suggested a strict coupling between channel opening (gating) and permeation. The idea that the selectivity filter is the gate was therefore investigated by using Monte Carlo simulations. Gating is accomplished by allowing the filter to alternate stochastically between two conformations: a high-affinity state, which selectively binds K ions (but not Na ions) and traps them, and a completely nonselective, low-affinity state, which allows both Na and K ions to permeate. The results of these simulations indicate that affinity switching not only endows the selectivity filter with gating abilities, it also allows efficient permeation without jeopardizing ion selectivity. In this model, permeation and gating result from the same process.

Single-ion channel behavior is dominated by two main functional states, open and closed (1). In the open state, ion permeation is efficient, whereas in the closed state, ion flux rates are very small (2). Although it is clear that channels must undergo a conformational change when moving between the open and closed states, the exact mechanism and structural basis for this phenomenon remains incompletely understood. The structure that is directly responsible for opening the channel is referred to as the "gate." It is commonly thought to act by a trapdoor mechanism, preventing ions from moving through the pore in the closed state and moving out of the way during channel opening (3). A steric mechanism of action for the gate was suggested by early experiments in voltage-gated K channels showing that the accessibility of cytoplasmic blockers depended on the state of activation of the channel (4). Analysis of macroscopic currents in the *Shaker* K channel further strengthened the idea that there is a tight steric closure at the cytoplasmic entrance to the channel that is widened after channel activation (5). A cytoplasmic localization for the gate is also supported by crystal structures of several prokaryotic K channels, which revealed a tight cytoplasmic constriction in the closed KcsA K channel and a wide-open internal vestibule in the "opened" calcium-activated MthK channel (6, 7). Finally, EPR spectroscopy measurements in KcsA revealed rotational movements of TM2 after activation and a subsequent widening of the cytoplasmic constriction (8). In this paradigm, permeation and gating are controlled by two structures at opposite ends of the permeations pathway. The selectivity filter localized at the external entrance to the pore determines ion selectivity and sets permeation rate, while a cytoplasmic constriction acts as a steric gate.

An alternative hypothesis for the nature of the gate has emerged from the analysis of so-called subconductance levels in the voltage-gated drk1 (Kv2.1) K channel (9–11). Whereas ion channels spend most of their time in the closed or open state, careful inspection of patch clamp recordings invariably reveals the existence of current levels that are intermediate between these two main states. In the drk1 K channel (11), as well as in other channels (12–14), these sublevels are visited during transitions between the open and closed state. Because the occurrence of sublevels strictly coincides with the movement of the gate, a strong coupling between permeation and gating is implied. We have therefore proposed that the same structure that controls permeation is also responsible for opening the channel (11). This structure is likely the selectivity filter, because the ion selectivity of subconductance levels is different from the main open state (15). The hypothesis that the selectivity filter is also the gate is supported by additional experimental data. Conservative point mutations in the selectivity filter have substantial effects on open state stability, a primary single-channel gating characteristic (15–17), whereas mutations at the cytoplasmic construction only affect bursting kinetics (18). Open state stability is determined by the permeating ion species, directly linking gating to selectivity (19, 20). Finally, in inwardly rectifying K channels, internal Ba^{2+} could access its binding site when the channel was closed, indicating that the gate lies within the selectivity filter (21).

If the selectivity filter functions as the gate, as our hypothesis suggests, then what is the gating mechanism? We have previously proposed that ions could be prevented from translocating in the closed conformation by binding to a high-affinity site, whereas reducing the depth of this energy well would enable ion permeation (11). In this scenario, the filter gates the channel by affinity switching. Here, this gating mechanism is investigated by using Monte Carlo simulations. The results reveal that a gated selectivity filter allows the channel to obtain high ion selectivity without jeopardizing efficient ion permeation.

Methods

A Monte Carlo simulation algorithm was written in FORTRAN-77 to evaluate a model of an ion channel containing an affinity-switching selectivity filter. A two-dimensional compartment is subdivided by a model membrane containing the selectivity filter (Fig. 1). K and Na ions are introduced in the top compartment at random positions and with random initial velocities. Their positions are updated every simulation step, by moving them to another position that is determined by their velocity vectors. If an ion leaves the compartment, it is replaced with a similar ion at a random position and given a new random velocity. If an ion reaches the membrane, it bounces back into solution. As a result, the concentration of K and Na ions remains constant. What happens when an ion arrives at the selectivity filter entrance depends on the state of the filter and the ion species. When the filter is occupied, both K and Na ions bounce back into solution. When the binding site in the filter is free, the affinity state of the filter determines the fate of the ion. In the low-affinity state, K ions are allowed to bind, but Na ions are not. Bound K ions

*To whom correspondence should be addressed. E-mail: vando005@mc.duke.edu.

www.pnas.org/cgi/doi/10.1073/pnas.0308743101

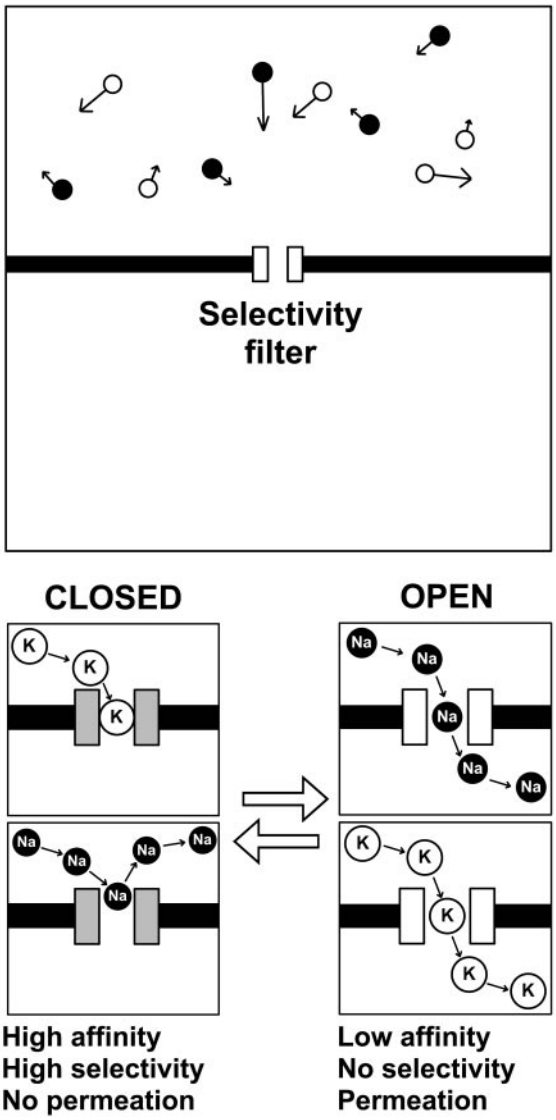

Fig. 1. Monte Carlo simulation of an affinity-switching selectivity filter. (*Upper*) The simulation environment consists of two compartments separated by a membrane containing a selectivity filter. Na and K ions move around stochastically and arrive at the entrance to the filter at random times. Whether these ions enter the filter depends on the ion species and filter state. (*Lower*). The selectivity filter functions as a gate by switching between two conformations, high affinity (closed) and low affinity (open). In the high-affinity state, only K ions are allowed to bind, but when bound, they remain trapped. This state therefore has high ion selectivity but does not support ion permeation (see Movie 1, which is published as supporting information on the PNAS web site). In the low-affinity state, both Na and K ions can enter the filter and both are allowed to diffuse out. Ions exit the filter to either the top or bottom compartment, which is determined by chance and with equal probability: ions have no memory. The low-affinity state has no ion selectivity, but ions permeate efficiently (see Movies 2 and 3, which are published as supporting information on the PNAS web site). In fact, permeation rate in the low-affinity state is limited by diffusion only. The software that was used to run the Monte Carlo simulations can be accessed and downloaded at www.vandongen-lab.com.

remain trapped until the filter moves to the low-affinity state. In the low-affinity state, both K and Na ions can enter the filter and dissociate from it readily. Ions have no memory, so they dissociate to the top and bottom compartments with equal probability. The filter stochastically alternates between high- and low-affinity states.

Results

The exquisite ion selectivity displayed by some channels implies that the ion-binding sites in their selectivity filters have evolved to provide optimal physicochemical environments for the permeating ions. This is illustrated by the selectivity filter of KcsA, where two fully dehydrated K ions are each coordinated by eight carbonyl oxygens. Whereas the coordination sphere appears to be perfect for K ions, the oxygens are too far apart to accommodate the smaller Na ion (6). Optimal coordination implies that permeant ions are bound with high affinity, which substantially reduces their dissociation rate. A major problem is therefore to understand how ion channels achieve high ion selectivity without jeopardizing efficient permeation. One solution is to use multiple binding sites, in which destabilizing ion–ion interactions increase the dissociation rate (22). Here, an alternative mechanism is investigated in which the conformation of the filter and the properties of the binding sites are dynamic.

Monte Carlo simulations of a K-selective channel were used to explore the idea that the selectivity filter can function as a gate by alternating between two states that differ in their K affinity. The simulation environment is described in *Methods* and Fig. 1. The goal of this very simplistic diffusion model is to simulate the stochastic arrival of Na and K ions at the entrance of the selectivity filter. Exactly how ions behave in solution is not important, as long as the arrival statistics are reasonable. Ion–ion interactions and the effect of water molecules on the ion trajectories were therefore not modeled. During the simulation, the filter stochastically alternates between two states, with high and low affinity for K ions.

The high-affinity state corresponds functionally to the closed state of the gate: permeant ions are bound with high affinity and consequently dissociate from the filter very slowly. Nonpermeant ions bind poorly, thus the high-affinity state is very ion-selective. In the simulations, it was assumed that the high-affinity state selectively binds K ions that arrive at the entrance and that the affinity is high enough that a bound K ion cannot dissociate during the lifetime of the state. Na ions that enter the selectivity filter entrance while it is in the high-affinity state are not able to bind and return back into solution.

The low-affinity state of the filter corresponds to the open state: ions inside the filter bind poorly and dissociate rapidly. Because the filter does not interact strongly with any ions in this state, it has to be poorly ion selective. In the simulations, the low-affinity state has no ion selectivity at all. The properties of the two filter states were made extreme to prevent the model from producing trivial results. When the simulations are run with the filter fixed in the high-affinity state, there is no permeation. The first K ion that reaches the filter binds and remains trapped. Because the binding site in the filter remains occupied, all ions that reach the filter bounce back into solution. Conversely, when the filter is fixed in the low-affinity state, permeation is efficient but there is no selectivity at all.

Next, Monte Carlo simulations were performed for a selectivity filter containing a single K-binding site, which stochastically alternates between a low- and high-affinity state. A key parameter is the relative amount of time the channel spends in each state. Simulations in which the filter spends most of its time in the low-affinity (open) state produce very poor ion selectivity, due to the nonselective nature of the low-affinity state. Consequently, as the probability of being in the low-affinity state (P_{low}) decreases, the ion selectivity of the channel increases. When P_{low} is 0.1, the channel permeates K ions 10 times better than Na ions. Therefore, affinity switching produces K-selective channels by functionally combining the ion selectivity of the high-affinity state with the permeation capabilities of the low-affinity state.

However, there could be a potential problem. To make the ion selectivity physiological relevant, the K/Na flux ratio needs to be

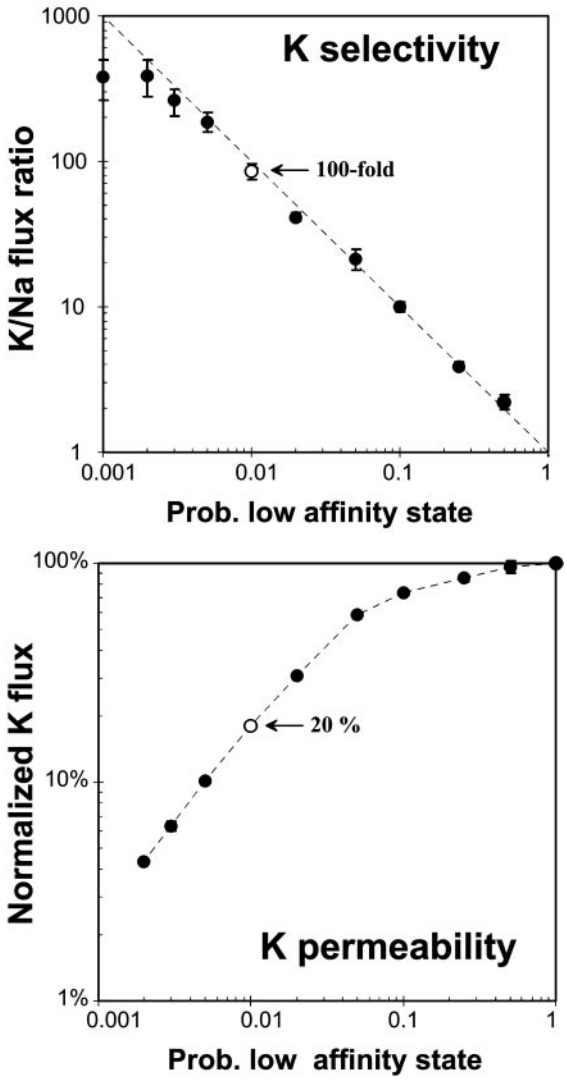

Fig. 2. Results for the one-site model. Monte Carlo simulations were performed for a model containing a single K-binding site. Gating kinetics were varied by setting the probability to be in the low-affinity state. Ten simulations were performed for each condition, and the mean and SE were calculated for the Na and K fluxes. Movies 4–6, which are published as supporting information on the PNAS web site, illustrate the simulations. (*Upper*) Ion selectivity, measured as the K/Na flux ratio, is plotted as a function of the probability to be in the low-affinity state (P_{low}). (*Lower*) The K flux rate for each value of P_{low} was normalized by dividing with the K flux rate obtained when the filter was fixed in the low affinity-state (the diffusion limit) and plotted against P_{low}. Note that 100-fold ion selectivity was achieved with a relative K flux that is 20% of the diffusion limit (○).

100 or better. This requirement implies that the channel spends virtually all of its time (>99%) in the high-affinity state, in which ions are trapped and block the channel, potentially resulting in unacceptably low permeation rates. This putative problem was investigated by running Monte Carlo simulations for a wide range of P_{low} values, counting total number of permeating Na and K ions and calculating the K/Na flux ratio. Potassium permeability rates were normalized by dividing the K ion flux rate in an affinity-switching experiment by the diffusion-limited K ion flux rate obtained with the filter locked in the open, low-affinity state. Fig. 2 illustrates the relationship between K ion selectivity and relative K permeation rate for the one-site model. Surprisingly, as ion selectivity increases with decreasing P_{low}, there is only a moderate penalty on permeation rate. For instance, a hundred-fold increase in ion selectivity is achieved with a permeation rate that is only 5-fold lower than the diffusion limit. This is a remarkable result for a model with only a single binding site.

Selectivity filters of real K channels employ multiple K-binding sites. The Monte Carlo simulations were therefore extended to a model containing two K-binding sites. Each site was gated independently, and bound K ions were allowed to jump to a neighboring site when it was not occupied by another ion. Bound Na ions were only allowed to move to a neighboring site when it was in the low-affinity state. Initially, the simulations were run, assuming the ions do not affect each other when both sites are occupied. The results were similar as for the one-site model, except now the ion selectivity, measured by the K/Na flux ratio, was inversely proportional to the product of the probabilities of being in the low-affinity state associated with the two sites. This can be seen in Fig. 3, which shows the result of simulations in which the two probabilities were made identical and varied over a wide range. With two identical sites, the ion selectivity depends very steeply on the probability of being in the low-affinity state: a P_{low} of 10% results in a K/Na flux ratio of 100. When P_{low} was decreased further, the ion selectivity kept increasing as P_{low}^{-2} but the relative flux rate decreased severely (Fig. 3). At these small P_{low} values, the filter is almost always doubly occupied, forcing ions to return back into solution instead of moving to the next site, thereby inferring with efficient permeation.

To try to relieve the filter clogging problem, a new set of simulations was performed, in which ions in a doubly occupied filter experience electrostatic repulsion. This process was implemented by forcing the binding sites to move to the low-affinity state when they are both occupied. The results of these simulations are shown in Fig. 4. Ion selectivity is still proportional to P_{low}^{-2}, but now the relative flux rate decreases minimally with increasing selectivity (Fig. 4): 1,000-fold K selectivity is achieved at a permeation rate that is only 3-fold below the diffusion limit.

Discussion

Monte Carlo simulations were presented to show that affinity switching allows a selectivity filter to function as a gate. The channel is functionally closed when the filter is in a high-affinity state because K ions are trapped. High-affinity binding sites for Ca and K ions have been experimentally demonstrated for voltage-gated Ca and K channels, respectively (23–26). In inwardly rectifying K channels, short-lived closed states result from K ions getting trapped inside the pore (27), indicating the existence of a K-binding site that it is capable of gating the channel.

In the model proposed here, ion selectivity results from the existence of a high-affinity state, in which the filter interacts strongly with the bound ion. As long as the channel remains in this high-affinity state, it remains functionally closed. Channel opening is achieved by allowing the filter to briefly visit a low-affinity state, which necessarily has reduced ion selectivity. In the simulations described here, ion selectivity was completely removed in the low-affinity state. The Monte Carlo simulations have shown that in order for the affinity-switching filter to display reasonable ion selectivity, it must spend most of its time in the high-affinity conformation. The low-affinity state therefore behaves as a transition state. This finding implies that during an open time interval observed in a single-channel recording, the filter is actually continuously, but very briefly switching to the low-affinity state, while during the closed time intervals it is locked in the high-affinity state (Fig. 5). The affinity switching described here is therefore very fast compared with the kinetics of single-channel gating. What exactly determines whether the filter is locked in the high-affinity state (producing a closed dwell

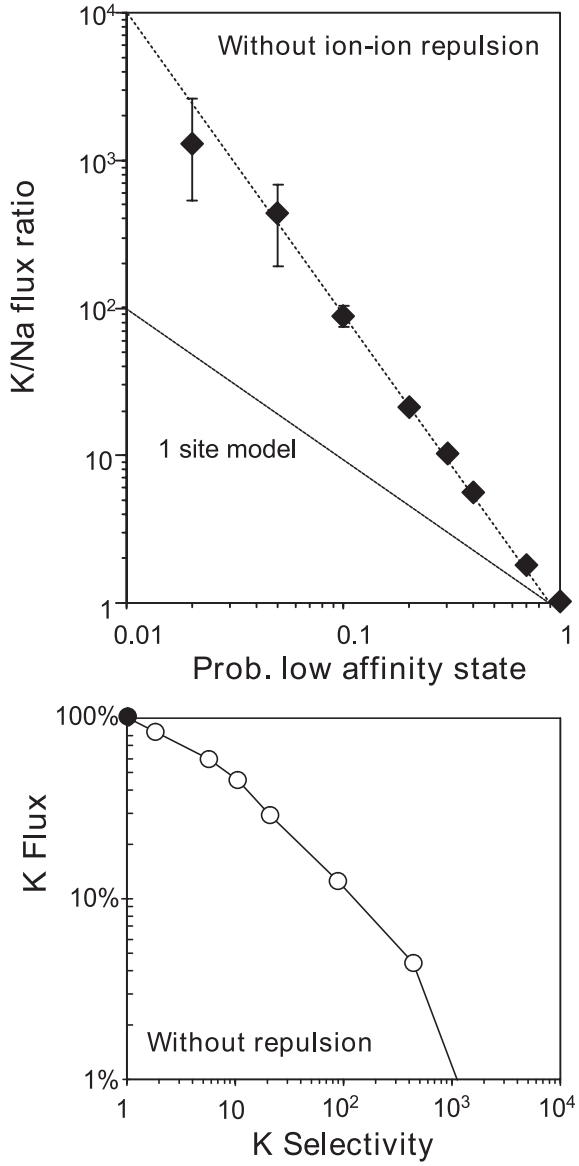

Fig. 3. Results for the two-site model lacking ion–ion interactions. Monte Carlo simulations were performed for a model containing a two identical K-binding sites. Gating kinetics were varied by setting the probability to be in the low-affinity state to the same value for each site. Ten simulations were performed for each condition, and the mean and SE were calculated for the Na and K fluxes. (*Upper*) Ion selectivity, measured of the K/Na flux ratio, is plotted as a function of the probability to be in the low-affinity state (P_{low}). (*Lower*) The K flux rate was normalized as described in Fig. 3 and was plotted against K selectivity (K/Na flux ratio).

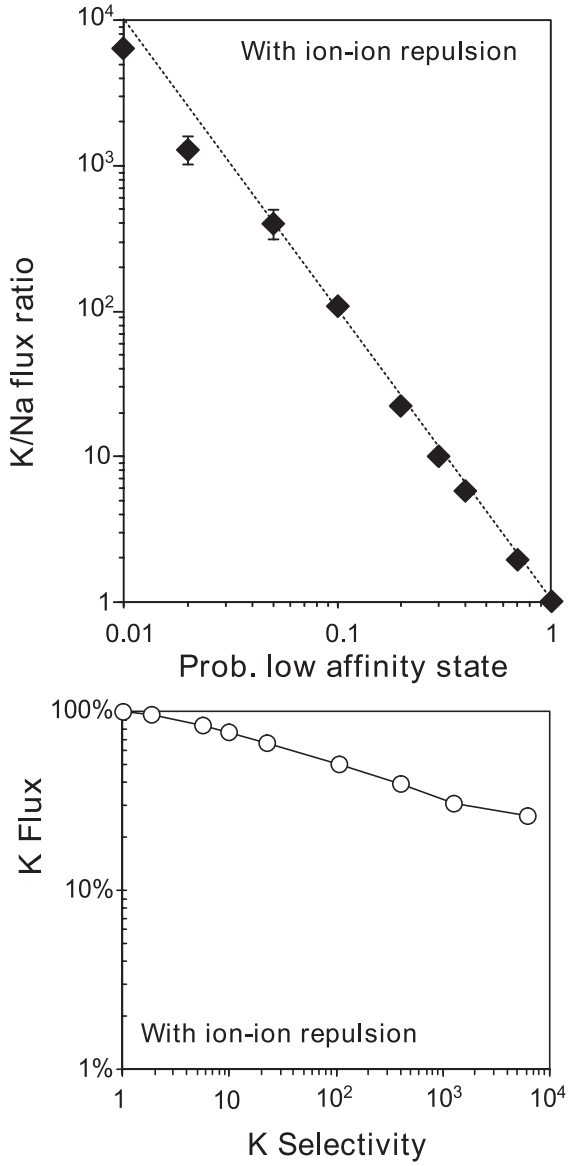

Fig. 4. Results for the two-site model with ion–ion repulsion. The simulations described in Fig. 3 were repeated allowing ion–ion repulsion. The ion selectivity as a function of P_{low} is not affected (*Upper*), but the relative flux rate decreases very little with increasing ion selectivity (*Lower*).

time) or is allowed to visit the low-affinity state (producing an open dwell time) is an important question that will require additional study.

What makes the affinity-switching mechanism so attractive is that very good ion selectivity can be achieved with minimal repercussions for the permeation rate, even for a channel containing only a single binding site. It is important to understand how this works. The filter acts as an efficient K ion catcher: it binds and traps any K ion that appears at its entrance. Consequently, the filter is virtually always occupied with a K ion. When it occasionally moves to the low-affinity state, it lets go of the ion that occupies it, which is almost always a K ion, because only K ions get trapped. The reason that the permeation rate does not get seriously degraded is that the channel spends most of its time waiting for a K ion to present itself at its entrance, where it is available to cross the membrane. As long as the average life time of the high-affinity state is not much longer than this waiting time, permeation will be relatively efficient.

What are the structural implications of this affinity-switching mechanism? If the low-affinity conformation is a transition state, as proposed here, then it has not been visualized in crystal structures. This result would imply that the filter structures seen thus far correspond to the high-affinity state. The near-perfect coordination chemistry seen for the K ions in the KcsA K channel filter certainly are not incompatible with a high affinity. The partial-negative charges of the eight carbonyl oxygens surrounding each K ion counteract its positive charge, which together with the water molecule that separates the two bound ions should substantial reduce, if not remove, electrostatic repulsion. Consequently, the two K ions in the KcsA filter appear to be bound very tightly, which is consistent with their well

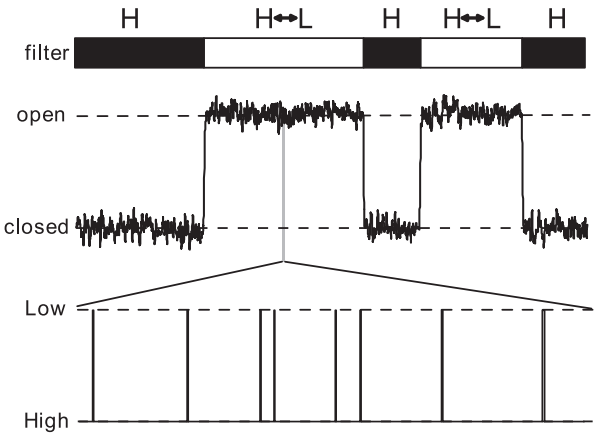

Fig. 5. Single-channel gating and affinity switching. A short segment of a single channel recording is shown in which the channel visits the open state twice. The bar above the current trace indicates the behavior of the selectivity filter, which is either locked in the high-affinity state H (filled bars), or it stochastically alternates between the high (H)- and low (L)-affinity states (open bars). (*Lower*) The diagram shows the behavior of the filter during an open interval at an expanded time scale: even when the channel is fully open, the filter spends most of its time in the high-affinity state.

defined crystallographic electron densities. Crystals are obtained at very low temperature and the perfectly symmetric oxygen cage of the filter is expected to get severely distorted at physiological temperatures due to the thermal movement of the atoms. Even a minimal increase (a fraction of an angstrom) in the average distance between the coordinating oxygens and the bound K ion will reduce the affinity by several orders of magnitude and allow the ion to escape from it binding site and eventually leave the channel. How this expansion of the oxygen cage is controlled is an important question that remains to be addressed.

The basic affinity-switching behavior described here must be allosterically controlled by other structures in the channel. The prime structural candidates are the four reentrant pore loops that form the selectivity filter, in particular the pore helices which provide the "spring-action" to keep the oxygen cage at an optimal conformation for coordinating K ions. A minimal rotation or translation of these helices would produce an expansion and distortion of the oxygen cage that would allow K ions to escape. The helices are also in physical contact with TM2 in KcsA, S6 in large K channels, and M3 in ionotropic glutamate receptors. Rotation of TM2/S6/M3 could therefore affect the conformation of the pore helices, thereby allosterically affecting the filter gate and produce more complex gating patterns (bursts, clusters of bursts, etc.) and adding different time scales. Mutations in S6 of positions in contact with the filter affect single-channel gating (28). The M3 segment in NMDA receptors rotates after ligand binding and acts as a transduction element, coupling ligand binding to channel opening, but it is functionally distinct from the gate (29).

The picture that emerges is a hierarchy of interacting structures that through a series of conformational changes set the free energy of the filter, which either allows visits to the low-affinity state (and permeation) or not (producing a wide variety of closed times). There is therefore no strict need for a steric mechanism to close the channel, although additional gates may certainly exist. Some channels, including KcsA and Shaker, contain a cytoplasmic constriction that would have to widen to allow ions to flow. Such a constriction therefore functions as a steric gate. However, many channels do not have a similar constriction. Examples include inward rectifier K channels (21) and ionotropic glutamate receptors (30), which have a similar pore forming structure as K channels (31). Of the three crystallized prokaryotic K channels (KcsA, MthK, and KvAP), only KcsA has a cytoplasmic constriction. The calcium-dependent MthK channel was crystallized in high calcium and has a wide-open internal vestibule, but there is currently no structure in low calcium to confirm that its vestibule is able to close. The voltage-dependent KvAP channel was crystallized with its voltage sensor domain in the resting position, but the cytoplasmic entrance is wide open (32).

Despite this variation in the extent to which the cytoplasmic entrance is constricted, the selectivity filters of these K channels show a remarkably consistent structure. It is proposed that the selectivity filter functions as a universal gate that opens and closes the channels by allosterically controlled affinity switching. The results from Monte Carlo simulations shown here suggest that permeation and gating are not only coupled, they are intimately linked into a single process.

This work was supported by National Institutes of Health Grants MH061506 and NS031557

1. Neher, E. & Sakmann, B. (1976) *Nature* **260,** 799–802.
2. Soler-Llavina, G. J., Holmgren, M. & Swartz, K. J. (2003) *Neuron* **38,** 61–67.
3. Hille, B. (1992) *Ionic Channels of Excitable Membranes* (Sinauer, Sunderland, MA).
4. Armstrong, C. M. (1971) *J. Gen. Physiol.* **58,** 413–437.
5. del Camino, D. & Yellen, G. (2001) *Neuron* **32,** 649–656.
6. Doyle, D. A., Cabral, J. M., Pfuetzner, R. A., Kuo, A., Gulbis, J. M., Cohen, S. L., Chait, B. T. & Mackinnon, R. (1998) *Science* **280,** 69–76.
7. Jiang, Y., Lee, A., Chen, J., Cadene, M., Chait, B. T. & Mackinnon, R. (2002) *Nature* **417,** 515–522.
8. Perozo, E., Cortes, D. M. & Cuello, L. G. (1999) *Science* **285,** 73–78.
9. VanDongen, A. M. J. & Brown, A. M. (1989) *J. Gen. Physiol.* **94,** 33A–34A.
10. VanDongen, A. M. J. (1992) *Comments Theor. Biol.* **2,** 429–451.
11. Chapman, M. L., VanDongen, H. M. A. & VanDongen, A. M. J. (1997) *Biophys. J.* **72,** 708–719.
12. Zheng, J. & Sigworth, F. J. (1998) *J. Gen. Physiol.* **112,** 457–474.
13. Schneggenburger, R. & Ascher, P. (1997) *Neuron* **18,** 167–177.
14. Ferguson, W. B., McManus, O. B. & Magleby, K. L. (1993) *Biophys. J.* **65,** 702–714.
15. Zheng, J. & Sigworth, F. J. (1997) *J. Gen. Physiol.* **110,** 101–117.
16. Chapman, M. L., Krovetz, H. S. & VanDongen, A. M. J. (2001) *J. Physiol.* **530,** 21–33.
17. Lu, T., Mainland, J., Jan, L. Y., Schultz, P. G. & Yang, J. (2001) *Nat. Neurosci.* **4,** 239–246.
18. Bichet, D., Haass, F. A. & Jan, L. Y. (2003) *Nat. Rev. Neurosci.* **4,** 957–967.
19. Spruce, A. E., Standen, N. B. & Stanfield, P. R. (1989) *J. Physiol.* **411,** 597–610.
20. LeMasurier, M., Heginbotham, L. & Miller, C. (2001) *J. Gen. Physiol.* **118,** 303–314.
21. Proks, P., Antcliff, J. F. & Ashcroft, F. M. (2003) *EMBO Rep.* **4,** 70–75.
22. Sather, W. A., Yang, J. & Tsien, R. W. (1994) *Curr. Opin. Neurobiol.* **4,** 313–323.
23. Ellinor, P. T., Yang, J., Zhang, J. F. & Tsien, R. W. (1995) *Neuron* **15,** 1121–1132.
24. Cloues, R. K., Cibulsky, S. M. & Sather, W. A. (2000) *J. Gen. Physiol.* **116,** 569–586.
25. Yang, J., Ellinor, P. T., Sather, W. A., Zhang, J.-F. & Tsien, R. W. (1993) *Nature* **366,** 158–161.
26. Korn, S. J. & Ikeda, S. R. (1995) *Science* **269,** 410–412.
27. Choe, H., Sackin, H. & Palmer, L. G. (2001) *J. Membr. Biol.* **184,** 81–89.
28. Liu, Y. & Joho, R. H. (1998) *Pflügers Arch.* **435,** 654–661.
29. Jones, K. S., VanDongen, H. M. A. & VanDongen, A. M. J. (2002) *J. Neurosci.* **22,** 2044–2053.
30. Beck, C., Wollmuth, L. P., Seeburg, P., Sakmann, B. & Kuner, T. (1999) *Neuron* **22,** 559–570.
31. Wood, M. W., VanDongen, H. M. A. & VanDongen, A. M. J. (1995) *Proc. Natl. Acad. Sci. USA* **92,** 4882–4886.
32. Jiang, Y., Lee, A., Chen, J., Ruta, V., Cadene, M., Chait, B. T. & Mackinnon, R. (2003) *Nature* **423,** 33–41.